



Short Communications

Coordination within paraspinal muscles during bipedalism in humans, a white-handed gibbon, and a Japanese macaque

Ryosuke Goto^{a, *}, Neysa Grider-Potter^{b, c}, Tetsuya Shitara^d, Yuki Kinoshita^e, Kenji Oka^f, Yoshihiko Nakano^d

^a Faculty of Rehabilitation, Gunma Paz University, 1-7-1 Tonyamachi, Takasaki, Gunma 370-0006, Japan

^b Department of Cell Systems and Anatomy, UT Health San Antonio, San Antonio, TX 78229, USA

^c Southwest National Primate Research Center, Texas Biomedical Research Institute, San Antonio, TX 78227, USA

^d Graduate School of Human Sciences, Osaka University, Suita, Osaka 565-0871, Japan

^e Primate Research Institute, Kyoto University, Inuyama, Aichi 484-8506, Japan

^f School of Rehabilitation, Osaka Kawasaki Rehabilitation University, Kaizuka, Osaka 597-0104, Japan

ARTICLE INFO

Article history:

Received 10 February 2022

Accepted 11 March 2023

Available online xxx

Keywords:

Hominoid

Macaque

Bipedal walking

Electromyography

Orthogrady

Paraspinal muscle

1. Introduction

Primate locomotor postures are classified as pronograde (horizontal trunk orientation) or orthograde (vertical trunk orientation; Nowak and Reichard, 2016). Orthograde bipedal walking and brachiation are unique in that they use only two limbs. Substrate reaction forces act on either the cranial portion of the trunk via the shoulder joint (brachiation), leaving the lower trunk free, or they act on the caudal portion of the trunk via the hip joint (bipedalism), leaving the upper trunk free. To control the motion at the free cranial or caudal portion of the trunk during locomotion, we hypothesize that a motor control system should intrinsically exist within the trunk because the action of the free limbs has a limited ability to maintain posture.

The trunk is balanced by intrinsic paraspinal muscles, and recruitment patterns of these muscles have been considered to be widely shared among extant hominoids during bipedalism (Shapiro

and Jungers, 1988) and anthropoids during quadrupedalism and bipedalism (Shapiro and Jungers, 1994). However, these studies analyzed the electromyograms (EMGs) of each intrinsic paraspinal muscle measured at a single vertebral level separately. Human EMG analyses have shown a temporally coordinated pattern in paraspinal muscle activation during bipedal walking (Prince et al., 1994; De Sèze et al., 2008; Ceccato et al., 2009). Prince et al. (1994) collected simultaneous surface EMGs recording paraspinal muscular activation at nine vertebral levels along the spinal column during human bipedal walking. They found a 'top-down' pattern in which the muscle fibers at cranial vertebral levels activated slightly earlier than those at caudal levels (Prince et al., 1994). The activation of human paraspinal muscles is temporally regulated across the vertebral levels, which might provide the upright spinal column with stability as a whole. However, no research has investigated intersegmental coordination within a paraspinal muscle in nonhuman primates. Therefore, the activation pattern in the back muscles shared among several anthropoids (Shapiro and Jungers, 1988, 1994) might result from unisegmental EMG measurements.

We hypothesize that orthograde hominoids (humans and gibbons) have an intrinsic motor control mechanism within the trunk because of a clade-based reliance on orthograde locomotion. We expect that hominoid paraspinal muscles will show the top-down activation pattern during bipedal walking but pronograde primates (macaque) will not. If pronograde primates show the top-down pattern, this would imply that minimal neural modifications accompanied the transition from quadrupedal to bipedal walking, as suggested by Shapiro and Jungers (1988, 1994).

2. Materials and methods

2.1. Sample

We simultaneously collected EMGs of one paraspinal muscle from five vertebral levels during bipedal walking in one female

* Corresponding author.

E-mail address: gotou@paz.ac.jp (R. Goto).

white-handed gibbon (*Hylobates lar*), one male Japanese macaque (*Macaca fuscata fuscata*), and eight male humans (*Homo sapiens sapiens*) with no histories of spinal disease ([Supplementary Online Material \[SOM\] Table S1](#)). This study conformed to the Declaration of Helsinki, and informed consent was obtained from all human participants according to the protocol of the Ethics Committee of Gunma Paz University (PAZ20-4). The animal experiments were conducted with approval from the Institutional Animal Care and Use Committee of Osaka University (26-10-2 and 27-3-2).

2.2. Nonhuman primate experiments

Electromyograms for the nonhuman primates were recorded using a wireless EMG system (BioLog DL-3000, S&ME Inc., Tokyo) with fine-wire electrodes (Stablonm 800B, California Fine Wire Co., California, USA). Under anesthesia (sevoflurane, Mylan Inc., Pennsylvania, USA), the fur was shaved and dry-heat-sterilized bipolar fine wires were inserted into the longissimus on the left side at the seventh cervical (C7), fourth, eighth, and twelfth thoracic (T4, T8, and T12, respectively), and fourth lumbar (L4) vertebral levels. Vertebral number was identified by counting and palpating the tips of the spinous processes. First, we identified the level of the last presacral vertebra (L5 in the hominoids; L7 in the macaque) by palpating the sacrum and vertebrae just above the sacrum. Next, we counted cranially until we reached C7. The spinous process of the seventh cervical vertebra, vertebrae prominens, is easily palpable in humans and our nonhuman primate sample. If our counts were inaccurate, we repeated counting the vertebrae until the C7 position was correctly identified. Intersegmental distances between the spinous processes were measured using a tape measure ([SOM Table S1](#)). Prior to locomotor experiments, we also dissected cadavers of a gibbon and a macaque of similar body mass to our living animals and measured the distance from the spinous processes to the boundary between longissimus and iliocostalis (~35 mm), which is palpable over the skin in our live experimental animals. We inserted the needles at the points 30 mm from the spinous processes, medial to the palpable boundary. After inserting the fine wires, the electrodes were stimulated using an oscillator (AD-8626, A&D Co., Ltd., Tokyo), which artificially contracted the muscle. Because trapezius, rhomboideus, and latissimus dorsi cover the paraspinal muscles, we verified lack of scapular and arm movement during electrical stimulation. Electrodes were connected to differential amplifiers (DL-140, S&ME Inc., Tokyo) and then to a 200 g telemetry transmitter. The transmitter was inserted into a pocket on the nonrestrictive jacket (Lomir Biomedical Inc., New York, USA) worn by the subjects.

After the subjects woke up, muscular activity was recorded at 1000 Hz. A synchronized digital camcorder (HDR-NX5J, Sony Corp., Tokyo) filmed the bipedal walking (frame rate of 59.94 fps) at a self-selected speed along a 7-m walkway on the concrete floor of the laboratory.

2.3. Human experiments

A motion capture system (Vicon Motion Systems Ltd., Oxford, UK) was used to collect EMG of the paraspinal muscles during bipedal walking at 2000 Hz; this was down-sampled to 1000 Hz to match the nonhuman primate data. The surface electrodes (Delsys Inc., Massachusetts, USA) were attached to the skin surface over the left longissimus at C7, T4, T8, T12, and L4. The L4 vertebra was sampled in all taxa, but L4 is more caudal in the lumbar region in humans and gibbons than in macaques. Following the same method we used for the nonhuman primates, the same vertebral levels were identified and the intersegmental distances between the spinous processes were measured ([SOM Table S1](#)). The surface

electrodes were placed at the points 10 mm away from the palpable boundary between longissimus and iliocostalis. The participants walked bipedally at their preferred speed without shoes along a 6-m walkway on the carpet floor in our laboratory. Lower limb touchdown and liftoff were identified based on the vertical components of the substrate reaction forces sampled at 2000 Hz (AMTI Inc., Massachusetts, USA). Because differentiating the surface EMG signals of longissimus from those of the other paraspinal muscles was difficult, from this point forward we use the term 'paraspinal muscles' for both the human and the nonhuman primates.

2.4. Data analysis

A gait cycle was defined as an interval between the sequential touchdowns of the left foot. Gait cycle duration and stance and swing phase durations were calculated by multiplying the number of interframe intervals during the phases by the duration of the interframe interval. The duty factors were calculated by dividing the stance duration of the left limb by the gait cycle duration. The duty factor was used as an indicator of the speed of bipedal walking because the space of the laboratory was not calibrated. Gait symmetry was computed by dividing the number of interframe intervals from the left limb touchdown to the right limb touchdown by the number of interframe intervals during the gait cycle. We selected the strides whose duty factors for right and left limbs were 0.5 or more, bilateral differences in the duty factors were 0.10 or less, and symmetry ranged from 0.45 to 0.55.

The EMGs were processed with a zero-lag band-pass Butterworth filter (50–500 Hz), notch Butterworth filter (50 and 60 Hz for the human and nonhuman primate signals, respectively), full-wave rectified, and smoothed by the zero-lag low-pass Butterworth filter (12 Hz). Amplitude was normalized using maximum amplitude at each vertebral level in the experimental session and expressed as percentages. The stride duration was not normalized; therefore, the time resolution of EMG profiles was 1 ms.

Cross-correlation analysis was used to determine the temporal shift of the EMG profiles in R v. 3.6.1 ([R Core Team, 2019](#)). The EMG profile at L4 was fixed, while those at the cervicothoracic vertebral levels were shifted toward phase advance and delay by 1 ms within a range (–200 to 200 ms). The cross-correlation coefficients were computed between the EMG profile at L4 and the shifted profiles at cervicothoracic levels. The magnitude of the shift at which the cross-correlation coefficient reached its maximum was defined as the temporal shift between L4 and cervicothoracic levels. The negative shift values represented muscle activation preceding the L4, i.e., leading, and positive values represented activation lagging behind L4.

2.5. Statistical analysis

Welch's t-tests were used to test for interspecific differences in the average duty factor. One-sample t-tests were used to assess whether the temporal shifts of EMG profiles relative to L4 were significantly different from zero. An ordinary least squares (OLS) multiple regression was conducted for each species using vertebral level (expressed as the intersegmental distance from L4) and the duty factor as independent variables and the shift relative to L4 as the dependent variable. Partial regression coefficients (PRCs) and standardized PRC (SPRCs) were also computed. Given the interspecific differences in gait cycle duration, another OLS linear regression was conducted for each species using the intersegmental distance from L4 as the independent variable and relative temporal shifts normalized by gait cycle duration (%gait cycle) as the dependent variable. All statistical analyses were conducted in R v. 3.6.1 ([R Core Team, 2019](#)). Statistical significance was set at $\alpha = 0.05$.

but adjusted to 0.017 using Bonferroni's correction for multiple interspecific comparisons of the duty factor.

2.6. Validation of the difference in the electrode type

To evaluate congruence between EMG methods, the muscular activities of the paraspinal muscles at L4 and T8 were simultaneously measured in 64 bipedal strides in the macaque by using both the surface (Vitrode F-150S, Nihon Kohden, Tokyo) and the fine-wire electrodes. Two surface electrodes were placed 25 mm from each other at each spinal level, and the fine wires were inserted at the midpoint between the surface electrodes. Through the same processes as the aforementioned method, temporal shifts at T8 and L4 between the surface and fine-wire EMG were determined. One-sample t-tests demonstrated that the temporal shifts were not significantly different between the surface and fine-wire electrode at each level, indicating that the results from the two types of electrodes are comparable (SOM Fig. S1; Table S2).

3. Results

In total, 575, 182, and 116 strides were obtained for the humans, gibbon, and macaque, respectively, showing significantly different average duty factors between the hominoids and macaque, in which the *p*-values were corrected by using the Bonferroni method (SOM Table S1; human vs. gibbon: $t = -1.85$, $df = 190.44$, $p = 0.07$; gibbon vs. macaque: $t = -8.01$, $df = 279.86$, $p < 0.01$; macaque vs. human: $t = 17.83$, $df = 131.38$, $p < 0.01$). The paraspinal muscles were primarily activated around the double support phase in all species (Fig. 1).

We observed the top-down pattern in the humans (except for C7) and in the gibbon, but not in the macaque (Fig. 2). In the humans, the average shift at C7 (-44 ms) did not precede that of T4 (-52 ms), suggesting that the top-down pattern was confined to the thoracolumbar spine in this study. On average, the humans and the gibbon showed negative shifts while the macaque showed positive shifts (Fig. 2; SOM Table S1), all but the macaque T8 were significantly different from zero (SOM Table S3).

Intersegmental distance from L4 and/or the duty factor variably influenced the activation shift depending on the species (Table 1). The PRCs in the multiple regression revealed that the distance from L4 significantly negatively influenced the shift in the humans and gibbon, but not significantly so in the macaque (Table 1). The duty factor significantly negatively influenced the shift in the gibbon and positively in the macaque, but not significant in the humans (Table 1). Therefore, with decreasing duty factor or increasing speed, the negative and positive shift values in the gibbon and the macaque, respectively, approached zero. For the gibbon, the SPRCs in Table 1 suggested that the intersegmental distance from L4 (-0.318) had a stronger influence on the shift than the duty factor (-0.111).

The single regression using the relative shift showed the slope for the gibbon (-0.0130) was similar to that of humans (-0.0134; Fig. 3; SOM Table S4), and the 95% confidence interval (CI) of the human slope (-0.0150 to -0.0119; SOM Tables S5) included the gibbon slope. The macaque slope (-0.0021; SOM Table S4) was not significant and fell outside the 95% CI of the human slope (SOM Tables S5).

4. Discussion

4.1. The top-down activation

We confirmed the top-down activation pattern of the paraspinal muscles in humans. Our results further suggest the presence of a

top-down activation pattern in the gibbon, but not the macaque. Because the gibbon pattern falls within the 95% CI of the human slope, we conclude that there is a similar temporal coordination of activation within the hominoid paraspinal muscles. Paraspinal muscle activation in this study is consistent with those previously reported for the thoracolumbar regions: muscles primarily activate during double support phases (Okada and Kondo, 1982; Thorstensson et al., 1982; Shapiro and Jungers, 1988, 1994; Higurashi et al., 2019). However, our human sample showed high background activity, especially at C7. Surface electrodes likely detected overlapping trapezius and rhomboideus muscles activity, which might mask the leading shift of the top-down pattern at C7. Trapezius profiles are easily differentiated from those of the paraspinal muscles because the major peak of the trapezius occurs at around 40% of the gait cycle, preceding the double support phase (Kuhntz-Buschbeck and Jing, 2012). Therefore, our general surface EMG profiles are accurate.

The temporally coordinated top-down pattern of the hominoid paraspinal muscles might provide mechanically balanced muscular tension over the long muscles. Paraspinal muscles are segmentally innervated by the dorsal rami of the spinal nerves in humans (Gray and Williams, 1995), anthropoids (Hartman and Straus, 1933; Miller, 1952), and other mammals (Fetcho, 1987) and a similar pattern is assumed for the gibbon. Generally, if muscle fiber contractions are not coordinated within a muscle, the tension generated by regional muscle fibers would only stretch adjacent regional muscle fibers and cannot efficiently act on skeletal elements (Loeb and Gans, 1986). Due to the segmental innervation pattern, intersegmental coordination of the paraspinal muscles is likely difficult and could result in unbalanced muscular tension if not appropriately coordinated. Because the muscular bundles constituting the paraspinal muscles attach to the cranial and caudal vertebrae of the spinal column (Diogo et al., 2012), we think that the top-down activation might be stabilizing the cranial vertebra first, in order to provide a stable base for these muscular bundles to effectively act on the caudal vertebra.

Because the macaque did not show this top-down pattern, we associate the observed pattern with the high frequency of upright trunk postures and/or innate bipedalism. The frequency of bipedal walking in wild gibbons (*H. lar*) has been reported to be 6.9% and all orthograde locomotor bouts is 80.9% for wild gibbons (Nowak and Reichard, 2016). The absence of a top-down pattern in the macaque suggests that the transition from quadrupedalism to bipedalism involved significant modifications to paraspinal muscle coordination.

4.2. Uniqueness of the human top-down pattern

The temporally coordinated activation in the human paraspinal muscles is robust against changes in duty factor, something unique to human upright bipedal walking. At the beginning of the double support phase, the touchdown of the contralateral hindlimb generates a backward substrate reaction force in the sagittal plane (Yamazaki, 1985; Ogiwara et al., 2018; O'Neil et al., 2022). The upper body lags behind the lower body due to inertia, which might produce a mechanical discrepancy between segments. In humans, the paraspinal muscles instantaneously activate at lower limb touchdown (Fig. 1), which might proactively mitigate the mechanical discrepancy before it is amplified. In the nonhuman primates, the paraspinal muscles might reactively activate in response to this discrepancy. The duration of the discrepancy should theoretically be proportional to the double support duration; therefore, if the discrepancy is proportional to the double support duration, this could account for the association between duty factor and size of the shift in the nonhuman primates (Table 1). On the other hand,

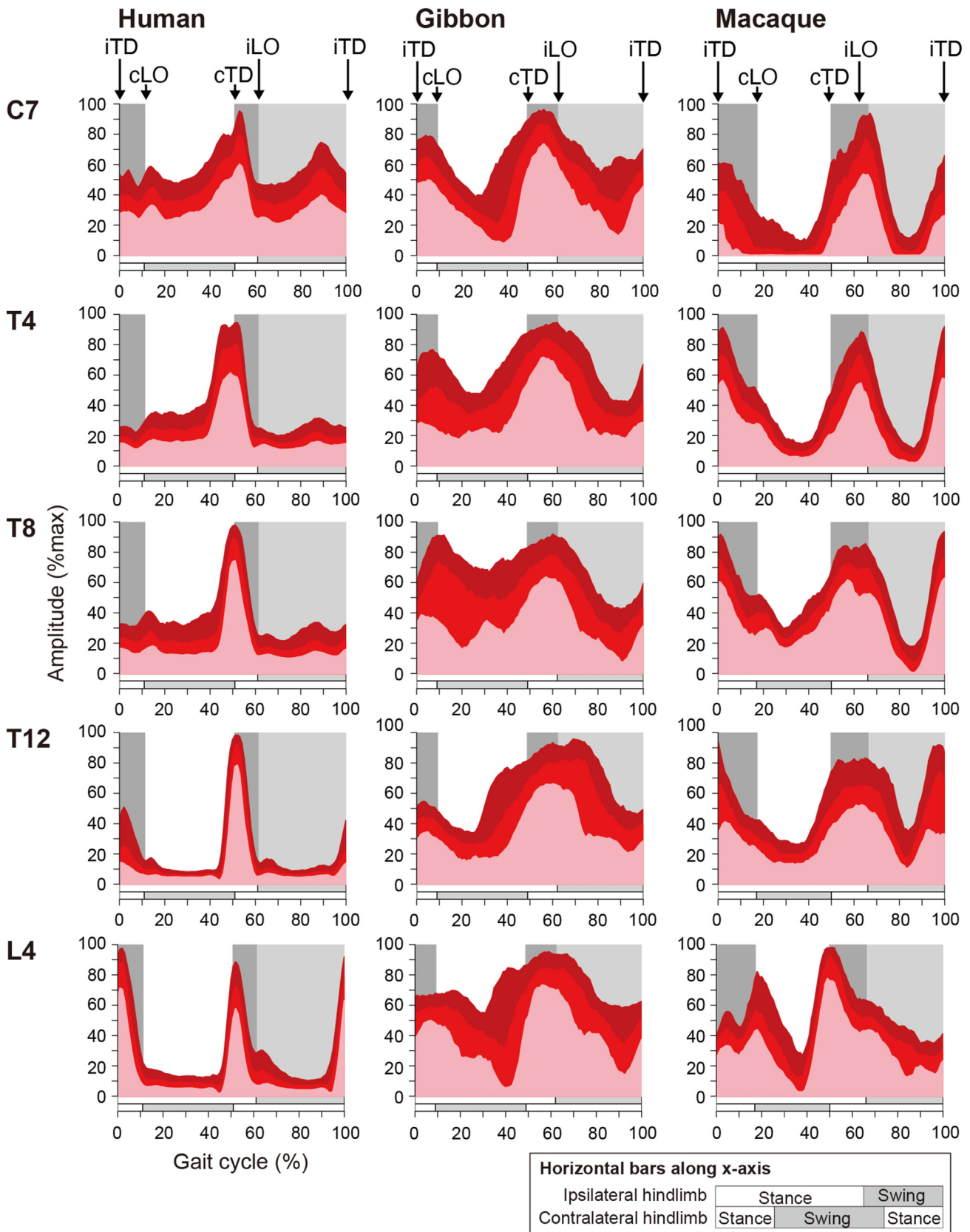


Figure 1. Activation of the paraspinal muscle during bipedal walking. The paraspinal muscle primarily activates around the double support phase. Electromyographic profiles are expressed as percentages relative to the maximum contraction experienced during the experiment at each vertebral level. Linear interpolation was used to normalize the stride duration. Percentiles demonstrate variation in activation patterns. Light pink represents 25th percentile of all muscular activations, red represents 50th percentile, and dark red represents 75th percentile. Light gray area in the background represents swing phase of the ipsilateral hindlimb; dark gray area represents double support phase. Abbreviations: iTD = ipsilateral hindlimb touchdown; iLO = ipsilateral hindlimb liftoff; cTD = contralateral hindlimb touchdown; cLO = contralateral hindlimb liftoff. (For interpretation of the references to color in this figure legend, the reader is referred to the Web version of this article.)

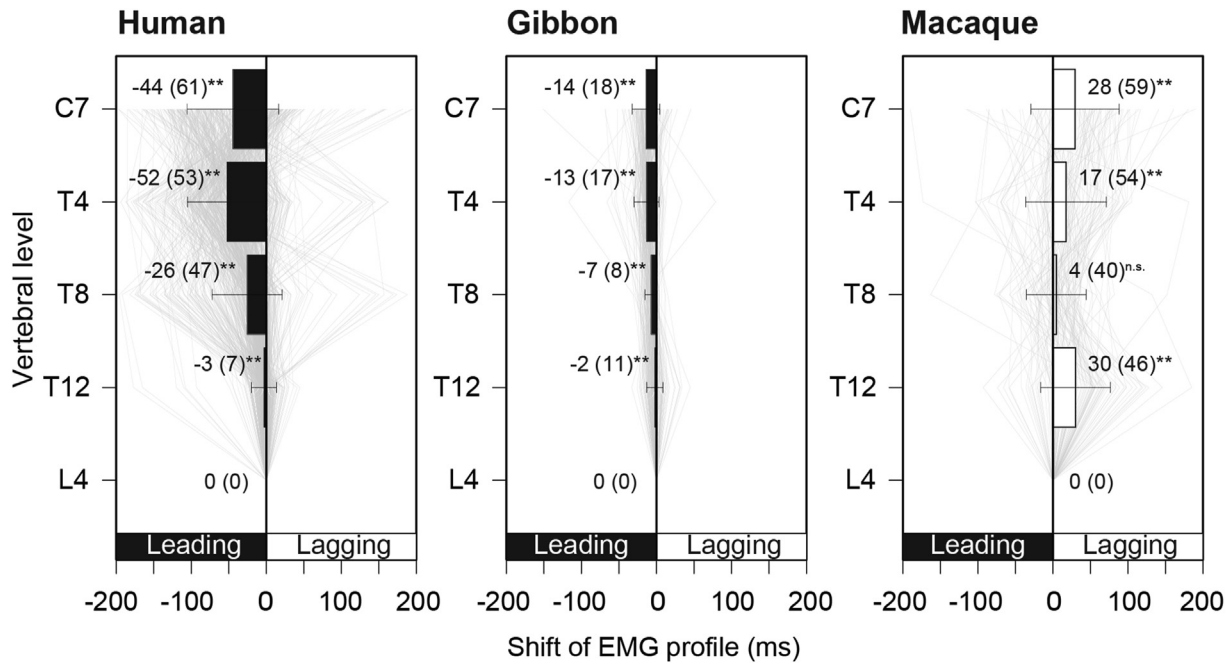


Figure 2. Average shifts of electromyographic profiles at cervicothoracic vertebral levels relative to L4. Minus and black bars represent profiles leading at vertebral levels relative to that of L4; plus and white bars represent profiles lagging. Values in parentheses represent standard deviations. ** = statistical significance at $p < 0.01$ in the one-sample t-test; * = statistical significance at $p < 0.05$; n.s. = nonsignificant. EMG, electromyogram.

Table 1

Results of multiple regression analyses for each species. Intersegmental distance from L4 (vertebral level) and duty factor are the independent variables and the shift relative to L4 is the dependent variable.^a

Species	Intersegmental distance from L4				Duty factor				Intercept				Regression significance	
	SPRC	PRC	SE	t-value	SPRC	PRC	SE	t-value	SPRC	PRC	SE	t-value	F value (df)	Adj. r^2
Human	-0.338	-0.15	0.01	-17.20	-0.005	-0.18	0.74	-0.24	0.000	20.92	46.37	0.45	148.2 (2, 2297)	0.11
Gibbon	-0.318	-0.08	0.01	-9.10	-0.111	-0.35	0.11	-3.17	0.000	25.52	7.08	3.60	46.4 (2, 725)	0.11
Macaque	-0.002	0.00	0.04	-0.05	13.230	2.95	1.03	2.87	0.000	-173.60	6.83	-2.54	4.11 (2, 461)	0.01

Abbreviations: SPRC = standardized partial regression coefficient; PRC = partial regression coefficient; SE = standard error; df = degrees of freedom; Adj. r^2 = adjusted r^2 .
^a Bolded values indicate significance at $p < 0.05$.

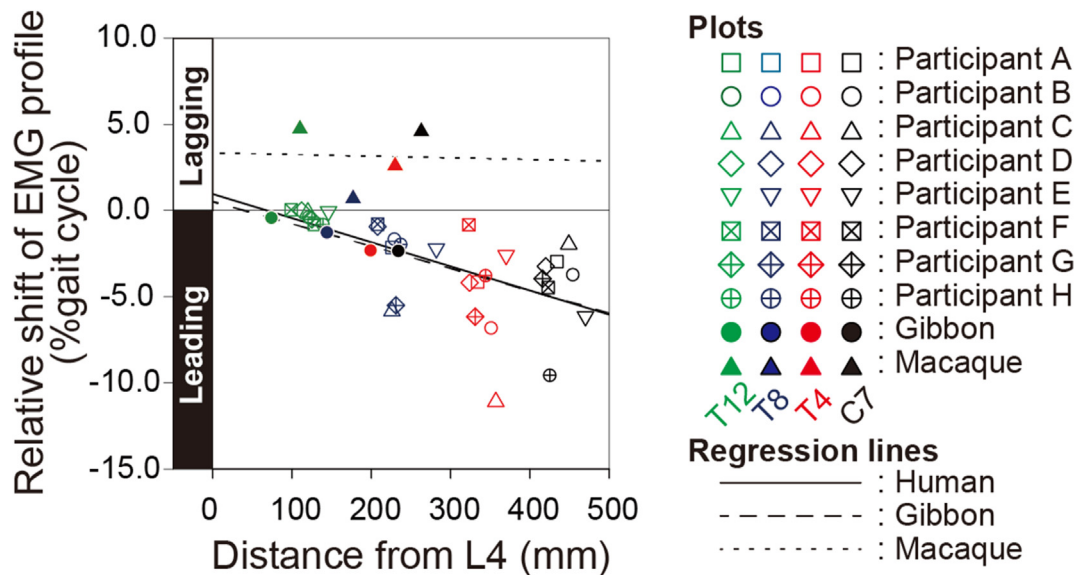


Figure 3. Bivariate plot of the least-squares single regression analyses for the humans, gibbon, and macaque with relative shift (%gait cycle) as the dependent variable and distance from L4 (mm) as the independent variable. EMG, electromyogram. (For interpretation of the references to color in this figure legend, the reader is referred to the Web version of this article.)

the proactive activation in humans results in no significant relationship between the shift and duty factor.

De Sèze et al. (2008) and Ceccato et al. (2009) suggested the existence of a complex neural circuit within the human central nervous system that produces the top-down pattern. If the top-down pattern is an indication of some neural basis, gibbons also have a similar mechanism; however, as the gibbon's top-down pattern is variable depending on changes in speed of bipedal walking, their neural system might somewhat differ from those of humans whose top-down pattern is independent of the duty factor (Table 1).

4.3. Limitations of the present study and future perspectives

Given that this study examined only one gibbon and one Japanese macaque, it is not possible to draw definitive conclusions regarding whether the top-down pattern can be generalized within gibbons or whether Japanese macaques never show this pattern. Investigating this pattern during bipedal walking in additional cercopithecoids would help to confirm if our results reflect a clade-based pattern. This study thus serves as the basis for future research that could provide indirect support for the relationship between bipedal walking and the unique activation of paraspinal muscles.

Our preliminary results indicated no significant influence of bipedal walking speed on the intersegmental temporal shift of activation in humans. As the participants in our study walked at preferred speeds, the multiple regression was based on a limited variance of the duty factor. Future studies should be directed toward investigating the robustness of the top-down pattern against locomotion speed using a large speed variance.

Author contributions

R.G., T.S., and Y.K. conceptualized and designed this study. R.G. conducted the experiments for the humans, R.G., N.G.P., K.O., and Y.K. for the gibbon, and R.G. and T.S. for the macaque. R.G. analyzed electromyographic data and wrote the initial draft of the manuscript. R.G., N.G.P., and Y.N. critically reviewed the manuscript. All authors gave their final approval for publication.

Conflict of interest statement

The authors have no financial conflicts of interest to disclose concerning this study.

Acknowledgments

We thank E. Hirasaki for his comments regarding our study and K. Otsubo and Y. Ichinose for their assistance in recording data. We would also like to thank Co-Editor-in-Chief A. Taylor, the Associate Editor, E. Vereecke, and two anonymous reviewers for helpful

comments and constructive critiques that improved the manuscript. This work was supported by Japan Society for the Promotion of Science, KAKENHI (grant number JP18K14804, to R.G.).

Supplementary Online Material

Supplementary online material to this article can be found online at <https://doi.org/10.1016/j.jhevol.2023.103356>.

References

- Ceccato, J.C., De Sèze, M., Azevedo, C., Cazalets, J.R., 2009. Comparison of trunk activity during gait initiation and walking in humans. *PLoS One* 4, e8193.
- De Sèze, M., Falgairolle, M., Viel, S., Assaiante, C., Cazalets, J.R., 2008. Sequential activation of axial muscles during different forms of rhythmic behavior in man. *Exp. Brain Res.* 185, 237–247.
- Diogo, R., Potau, J.M., Pastor, J.F., De Paz, F.J., Ferrero, E.M., Bello, G., Barbosa, M., Aziz, M.A., Burrows, A.M., Arias-Martorell, J., Wood, B.A., 2012. Photographic and Descriptive Musculoskeletal Atlas of Gibbons and Siamangs (*Hylobates*). CRC Press, Boca Raton.
- Fetcho, J.R., 1987. A review of the organization and evolution of motoneurons innervating the axial musculature of vertebrates. *Brain Res. Rev.* 12, 243–280.
- Gray, H., Williams, P.L., 1995. *Gray's Anatomy*. Churchill Livingstone, New York.
- Hartman, C.G., Straus Jr., W.L., 1933. *The Anatomy of the Rhesus Monkey (Macaca mulatta)*. The Williams & Wilkins Company, Baltimore.
- Higurashi, Y., Maier, M.A., Nakajima, K., Morita, K., Fujiki, S., Aoi, S., Mori, F., Murata, A., Inase, M., 2019. Locomotor kinematics and EMG activity during quadrupedal versus bipedal gait in the Japanese macaque. *J. Neurophysiol.* 122, 398–412.
- Kuhtz-Buschbeck, J.P., Jing, B., 2012. Activity of upper limb muscles during human walking. *J. Electromyogr. Kinesiol.* 22, 199–206.
- Loeb, G.E., Gans, C., 1986. *Electromyography for Experimentalists*. University of Chicago Press, Chicago.
- Miller, R.A., 1952. The musculature of *Pan paniscus*. *Am. J. Anat.* 91, 182–232.
- Nowak, M.G., Reichard, U.H., 2016. Locomotion and posture in ancestral hominoids prior to the split of hylobatids. In: Reichard, U.H., Hirai, H., Barelli, C. (Eds.), *Evolution of Gibbons and Siamang*. Springer Science+Business Media, New York, pp. 55–89.
- Ogihara, N., Hirasaki, E., Andreda, E., Blickhan, R., 2018. Bipedal gait versatility in the Japanese Macaque (*Macaca fuscata*). *J. Hum. Evol.* 125, 2–14.
- Okada, M., Kondo, S., 1982. Gait and EMGs during bipedal walk of a gibbon (*Hylobates agilis*) on flat surface. *J. Anthropol. Soc. Jpn.* 90, 325–330.
- O'Neil, M.C., Demes, B., Thompson, N.E., Larson, S.G., Stern, J.T., Umberger, B.R., 2022. Adaptations for bipedal walking: Musculoskeletal structure and three-dimensional joint mechanics of humans and bipedal chimpanzees (*Pan troglodytes*). *J. Hum. Evol.* 168, 103195.
- Prince, F., Winter, D., Stergiou, P., Walt, S., 1994. Anticipatory control of upper body balance during human locomotion. *Gait Posture* 2, 19–25.
- R Core Team, 2019. R: A language and environment for statistical computing. R Foundation for Statistical Computing, Vienna.
- Shapiro, L.J., Jungers, W.I., 1988. Back muscle function during bipedal walking in chimpanzee and gibbon: Implications for the evolution of human locomotion. *Am. J. Phys. Anthropol.* 77, 201–212.
- Shapiro, L.J., Jungers, W.I., 1994. Electromyography of back muscles during quadrupedal and bipedal walking in primates. *Am. J. Phys. Anthropol.* 93, 491–504.
- Thorstensson, A., Carlson, H., Zomlefer, M.R., Nilsson, J., 1982. Lumbar back muscle activity in relation to trunk movements during locomotion in man. *Acta Physiol. Scand.* 116, 13–20.
- Yamazaki, N., 1985. Primate bipedal walking: Computer simulation. In: Kondo, S. (Ed.), *Primate Morphophysiology, Locomotor Analyses, and Human Bipedalism*. University of Tokyo Press, Tokyo, pp. 105–130.